Electronic Supplementary Information

Layered Graphene/Mesoporous Carbon Heterostructures with Improved Mesopore Accessibility for High Performance Capacitive Deionization

Owen Noonan,[†] Yang Liu,[†] Xiaodan Huang,[†] Chengzhong Yu[*†]*

[†]Australian Institute for Bioengineering and Nanotechnology, The University of Queensland,

Brisbane, QLD 4072, Australia

Results and Discussion

(I) ionic influx coefficient versus concentration in CDI and EDLC:

The ionic influx coefficient (y-axis) is given by the ratio of influx ions during electrosorption/EDLC charge storage relative to the number of ions initially present in the flooded pore voids before adsorption/charging (equation 1). This influx coefficient indicates the magnitude of the positive influx necessary to equilibrate the adsorption/charge.

The ionic concentration in the pores is designated the same as in the bulk solution and the pore volume is assigned as 1 $cm^3\ g^{-1}$. Typical CDI capacity range of 10-20 mg g^{-1} is used to plot the correlation curves. The numbers of ions involved in CDI is calculated by equation 2. Typical EDLC capacitance range of 50-200 F g^{-1} is selected for plotting. The ion numbers involved in EDLC charge is calculated by equation 3.

The ionic influx coefficient (y-axis) calculation:

$$y = \frac{(total\ number\ of\ ions\ involved - number\ of\ initial\ ions\ present\ in\ pores)}{(number\ of\ initial\ ions\ present\ in\ pores)} \quad (1)$$

Number of ions involved in salt storage (CDI):

$$ions_{CDI} = \frac{SAC \times 10^{-3} \times N_A}{MW\ of\ NaCl} \quad (2)$$

Where, SAC is the CDI capacity (mg g^{-1}), N_A is the Avogadro constant ($6.022 \times 10^{23}\ mol^{-1}$), and the molecular weight of NaCl is 58.4 g mol^{-1}.

Number of ions involved in charge storage (EDLC):

$$ions_{EDLC} = C_{dl} \times Q_{1C} \quad (3)$$

Where, C_{dl} is the specific capacitance at the double layer (F g^{-1}) and Q_{1C} is the number of charges in one coulomb (6.242×10^{18}).

Number of ions initially present in pores (1 cm^3 g^{-1}):

$$ions_{pore} = c \times 10^{-3} \times N_A$$

Where, N_A is the Avogadro constant (6.022×10^{23} mol^{-1}), and c is the solution concentration (mol L^{-1}).

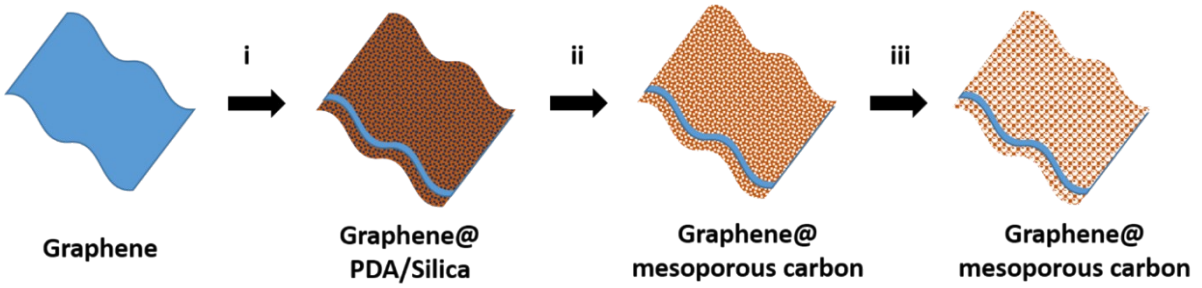

Figure S1. Formation process of G@MC materials. (i) Graphene is coated with a layer of PDA/silica nanocomposite using the *in-situ* Stöber templating method previously reported.[32] By Adjusting the amount of TEOS used from 1mL to 2mL, and the amount of graphene in suspension from 150 mg to 200 mg, layer thickness and pore opening can be controlled. (ii) Carbonisation and etching converts the PDA/silica composite to mesoporous carbon. (iii) Secondary thermal treatment enlarges pore openings on the surface of the composite.

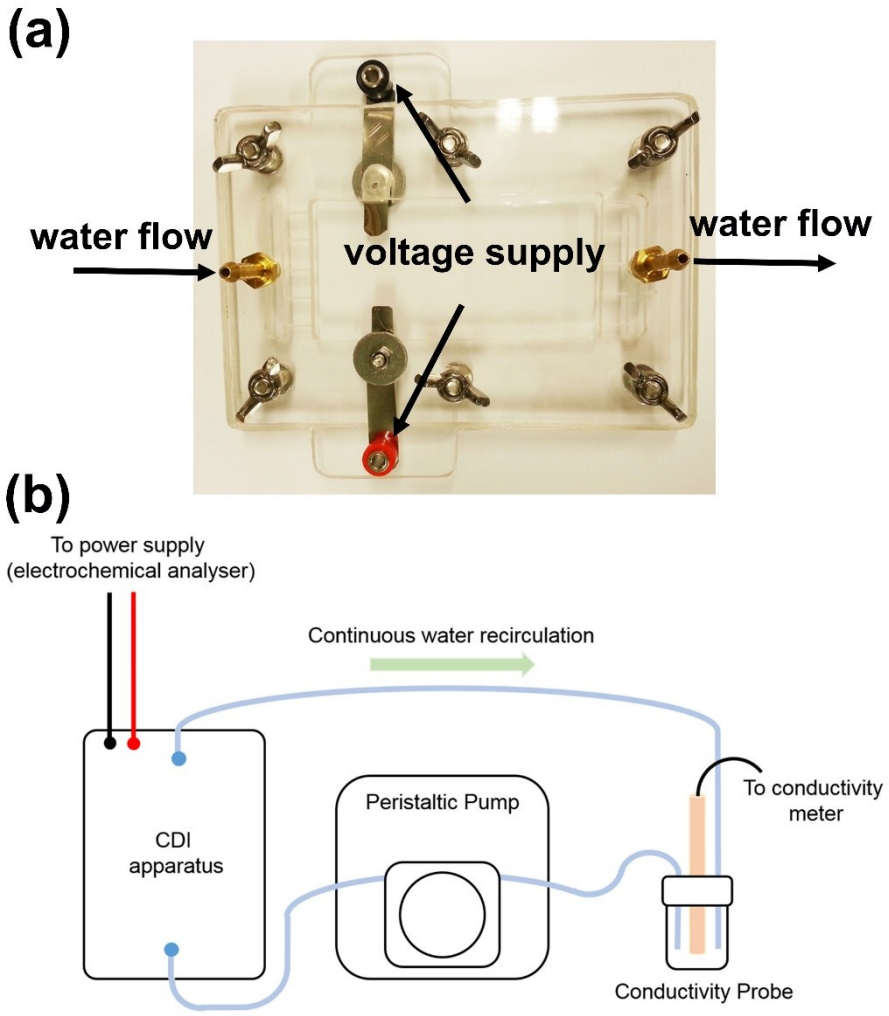

Figure S2. (a) Digital image of lab made flow-by CDI cell and (b) schematic diagram of CDI testing configuration. The flow rate is 25 mL min^{-1}.

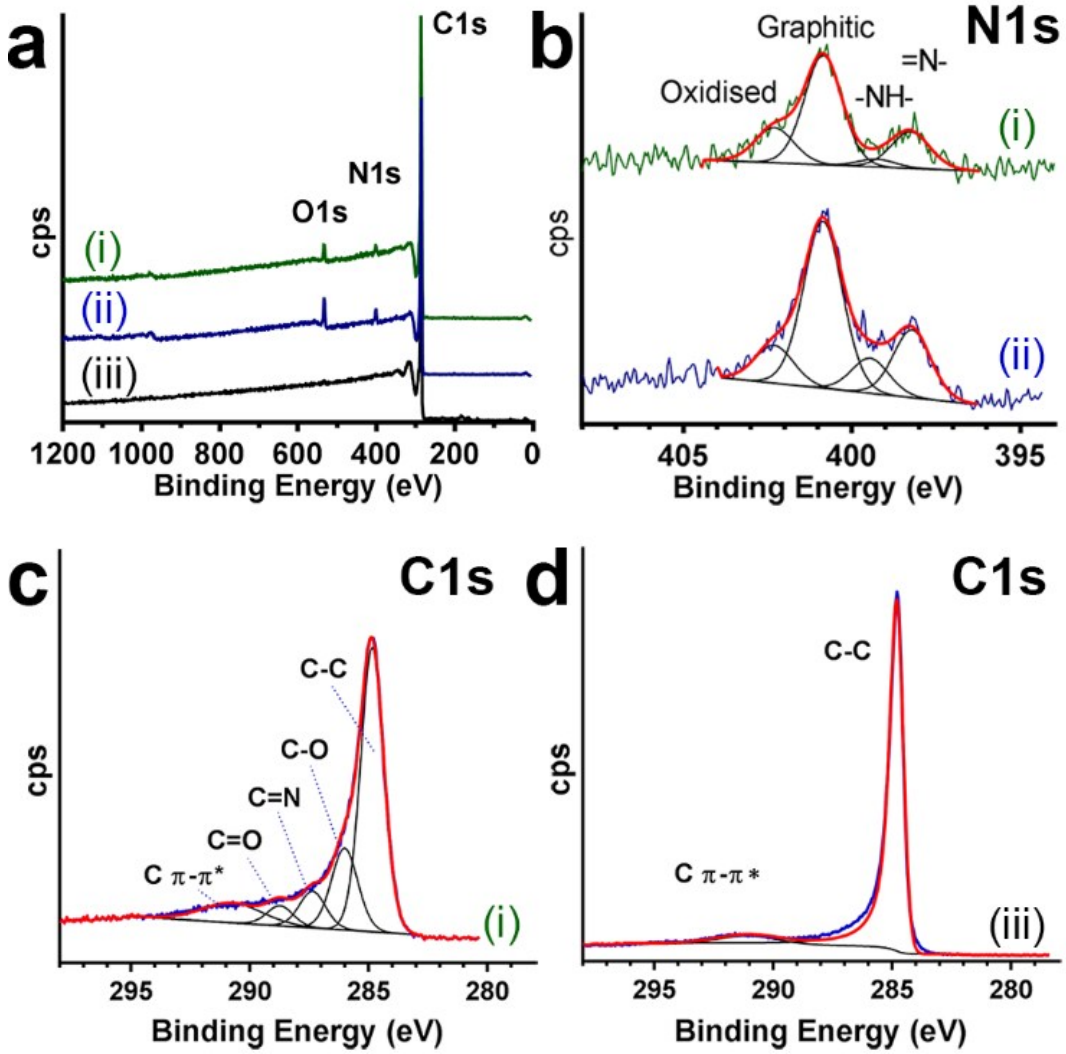

Figure S3. XPS survey scan (a) and high resolution scans of the N1s (b) and C1s (c,d) for G@MC-O-thin (i), G@MC-PO-thin (ii), and annealed graphene (iii).

Table S1. Elemental composition from XPS.

	N at. %	**O at. %**	**C at. %**	**Pyridinic N %**	**Pyrrolic N %**	**Graphitic N %**	**Oxidised N %**
G@MC-O-*thin*	4.2	5.2	90.1	19.7	4.1	57.2	19.0
G@MC-PO-*thin*	5.1	10.6	84.3	21.5	11.2	54.9	12.4
Graphene	0.0	0.7	99.3	-	-	-	-

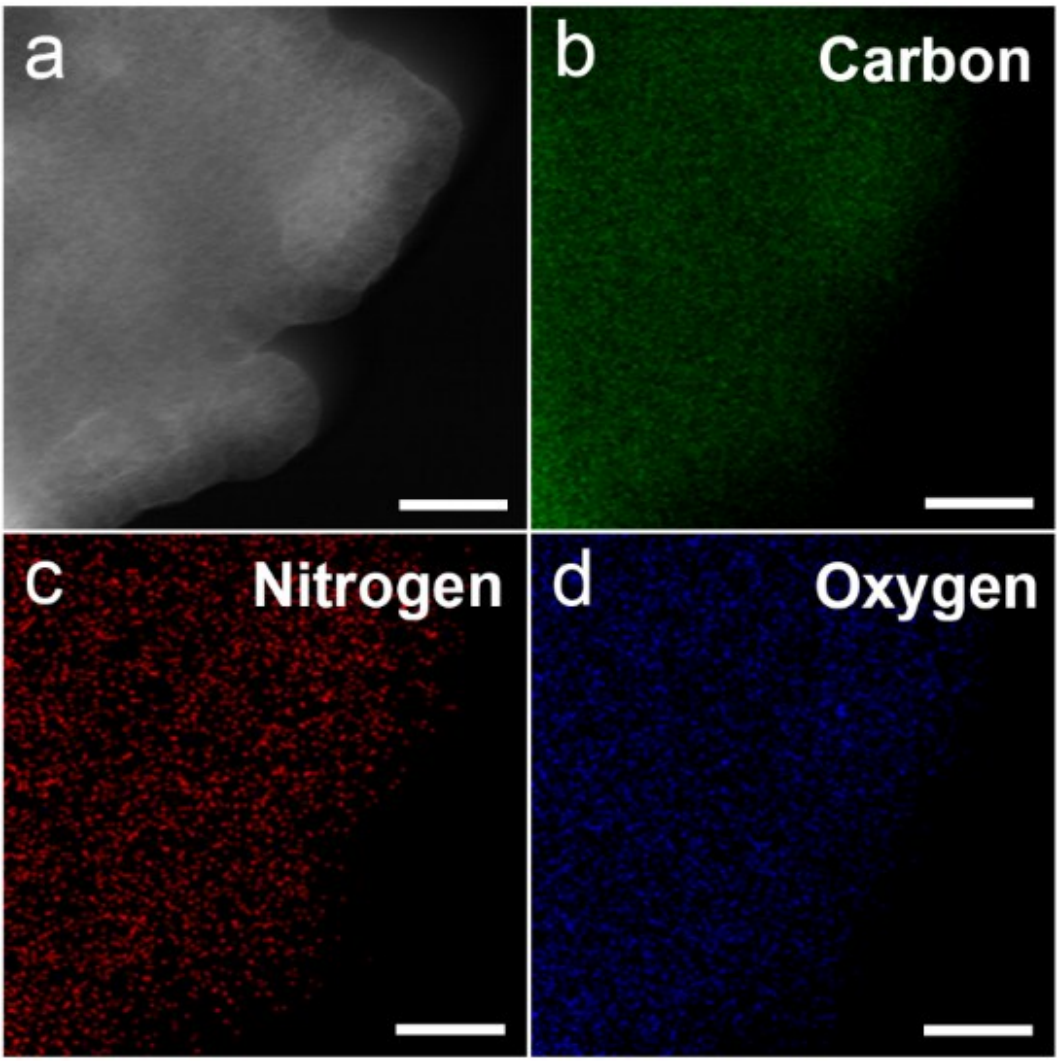

Figure S4. STEM HADDF image of G@MC-O-thin materials (a) and EDS elemental mapping of the same region showing carbon (b), nitrogen (c), and oxygen (d) distribution. Scale Bar: 100 nm.

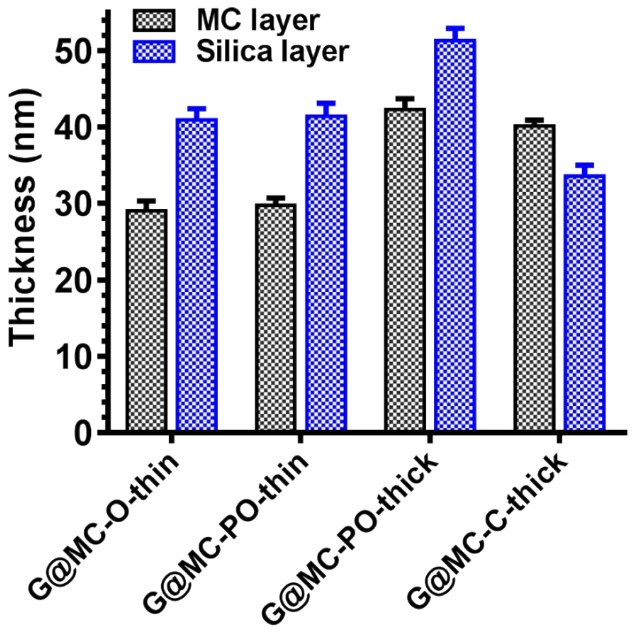

Figure S5. Mean layer thicknesses measured from TEM for the mesoporous carbon layer after carbonisation (black) and silica layer after calcination (blue) for the four samples. Error bars are taken from the standard deviation of over 20 measurements.

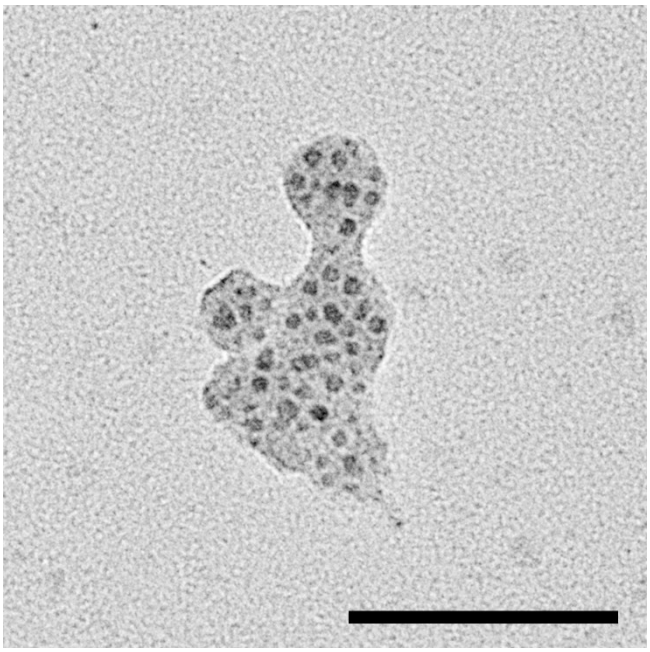

Figure S6. TEM image of secondary silica particles observable after washing G@SiO_2/PDA composites in NaOCl for samples prepared at high TEOS/PDA ratios (ie. G@MC-O-thin, G@MC-PO-thin and G@MC-PO-thick). Scale bar: 200 nm.

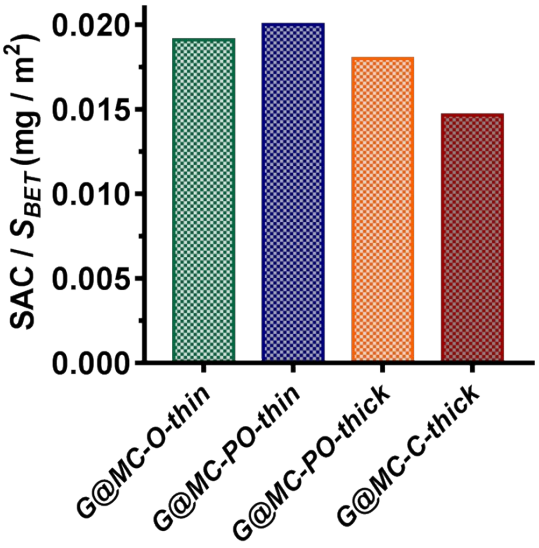

Figure S7. Salt adsorption capacity normalised by BET surface area for the four samples.

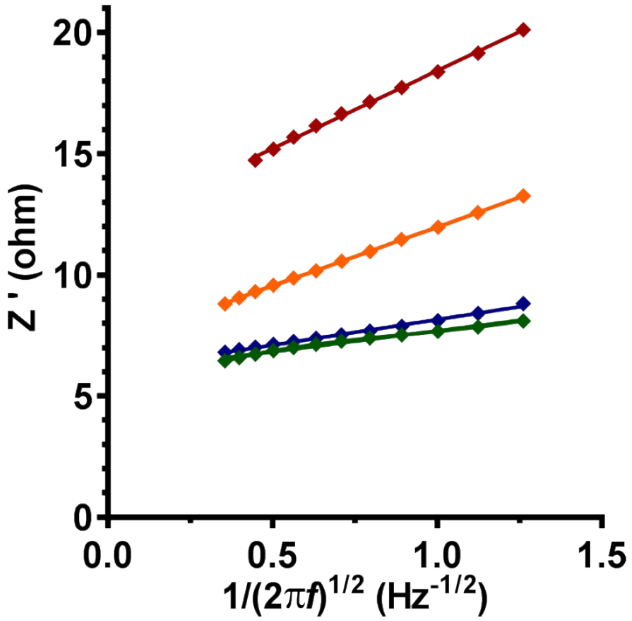

Figure S8. Warburg plots from low frequency region of Nyquist plot. G@MC-O-thin (green), G@MC-PO-thin (blue), G@MC-PO-thin (orange) and G@MC-PO-thick (red).

Table S2. Synthesis variables for G@MC materials.

	Graphene mg	TEOS mL	Dopamine hydrochloride mg	Activation
G@MC-C-thick	150	1	400	No
G@MC-PO-thick	150	2	400	No
G@MC-PO-thin	200	2	400	No
G@MC-O-thin	200	2	400	Yes

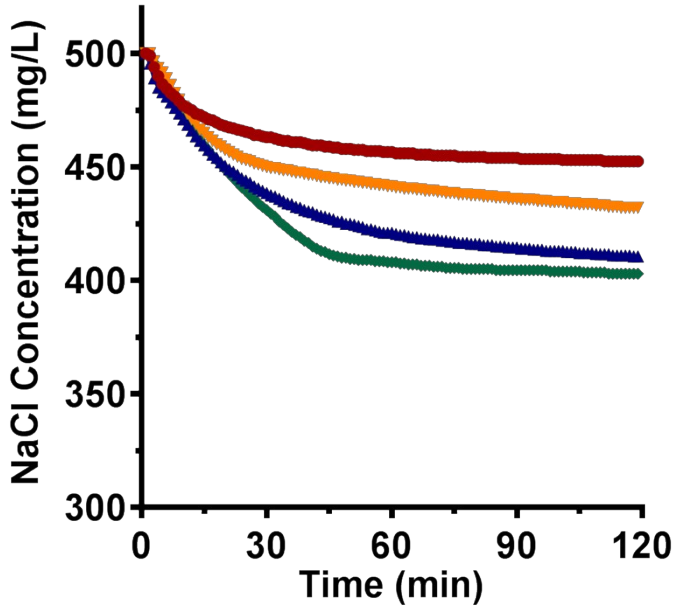

Figure S9. Concentration profiles for G@MC-O-thin (green ♦), G@MC-PO-thin (blue ▲), G@MC-PO-thick (orange▼) and G@MC-C-thick (red ●) in 500 mg L^{-1} NaCl, 25 mL/min at 1.5 V.